# A real-time optimal coordination scheme for the voltage regulation of a distribution network including an OLTC, capacitor banks, and multiple distributed energy resources

CrossMark

Khawaja Khalid Mehmood [a,*], Saad Ullah Khan [a], Soon-Jeong Lee [b], Zunaib Maqsood Haider [a], Muhammad Kashif Rafique [a], Chul-Hwan Kim [a]

[a] College of Information and Communication Engineering, Sungkyunkwan University, Suwon, Republic of Korea
[b] Economy and Management Research Institute, Korea Electric Power Corporation, Naju, Republic of Korea

ARTICLE INFO

ABSTRACT

The progression towards smarter grids, incorporating clean energy resources, has increased the integration of distributed generators (DGs) into power distribution networks. The DGs often cause a rise in voltage at their points of common coupling. Ordinary voltage regulation devices such as on-load tap changers (OLTCs) are not capable of addressing these issues adequately without careful coordination with DGs. In this paper, a new supervisory control and data acquisition-based two-stage voltage control scheme for the coordination of an OLTC transformer, capacitor banks (CBs) and the DGs is presented. The proposed scheme sets forth a new criterion for the selection of tap positions of an OLTC. In the first stage, tap positions of the OLTC are changed optimally using the micro genetic algorithm, whereas in the second stage, a recursive genetic algorithm is run to minimise the power losses in order to find the optimal reactive powers for the distribution network. Stochastic modelling of wind speed and solar irradiance data is also performed. The scheme is verified by studying it under four different test cases. An OLTC, CBs, photovoltaic panels, wind power DGs and dispatchable DGs are installed in the distribution network, and an IEEE 37-node test feeder is used for the verification of the proposed scheme. The simulation results show that the scheme achieves the objective of voltage regulation.

© 2017 Elsevier Ltd. All rights reserved.

## 1. Introduction

### 1.1. Motivation

Widespread awareness of global warming has catalysed the integration of various eco-friendly, zero-emission distributed generators with power grids. A large number of DGs have already been integrated with distribution networks, and a significant increase in this number is expected until 2050 [1]. The DGs pose a number of challenges to the protection devices in the traditional distribution systems [2,3]. Active distribution networks, the distribution networks with DGs, often encounter the problem of voltage rise at the points of common coupling of the DGs [4,5]. The problem of voltage rise can be traced to high DG penetration. Conventional voltage regulation devices such as OLTCs are sometimes unable to resolve these issues without proper coordination of different power equipment. Without the proper coordination between an

OLTC, CBs and various distributed energy resources, the number of switching operations in these devices rise significantly, thereby degrading the power quality. The absence of a rigorous coordination scheme suggests that the negative impacts of DG integration may outweigh the benefits.

IEEE Standard 1547 suggests that DGs cannot actively participate in the voltage regulation of the distribution network unless the distribution system operators (DSOs) require them to change their outputs based on the voltage control of a distribution system [6]. DGs should act as constant power resources to prevent the simultaneous interactions of various voltage control devices. With the integration of non-dispatchable DGs such as the wind and solar power DGs, optimal voltage regulation in real-time has become a challenging task. In the past, owing to long execution time of optimisation algorithms for large power systems, the schemes which were proposed as real-time voltage regulation schemes do not employ the optimisation algorithms. For the optimal operation of distribution networks, solutions in the form of day-ahead scheduling schemes were proposed. It has been mentioned in [7] that the severe errors of MW may occur in the forecasting due to

**Nomenclature**

*Acronyms*

| | |
|---|---|
| CB | capacitor bank |
| DG | distributed generator |
| DSPDG | dispatchable DGs |
| MAC | master controller |
| MCS | Monte Carlo simulations |
| MLE | maximum likelihood estimation |
| OLTC | on-load tap changer transformer |
| PF | power factor |
| PV | photovoltaic |
| RGA | recursive genetic algorithm |
| SAC | slave controller |
| SCADA | supervisory control and data acquisition |
| $\mu$-GA | micro genetic algorithm |

*Indices*

| | |
|---|---|
| $c$ | index of a CB |
| $d$ | index of DSPDGs |
| $i$ | index of system buses $\forall\, i \in N$ |
| $j$ | index of system buses $\forall\, j \in N$ |
| $s$ | index of PV panels |
| $t$ | index of time |
| $w$ | index of wind DGs |

*Variables*

| | |
|---|---|
| $\alpha_{n,n+1,\ldots,N}$ | samples generated from uniform distribution |
| $\gamma_s, \gamma_w, \gamma_d$ | PV panels, wind DGs and DSPDGs, respectively |
| $\lambda$ | tap position |
| $\lambda_{min}, \lambda_{max}$ | minimum and maximum value of the tap positions |
| $\Lambda$ | fill factor |
| $\phi_{(i,t)}$ | PF of the $i$-th DG at time $t$ |
| $\phi_{min}, \phi_{max}$ | minimum and maximum value for a PF |
| $\phi_w, \phi_s, \phi_d$ | PFs of a wind DG, PV panel and DSPDG |
| $\veebar$ | exclusive or operation |

| | |
|---|---|
| $C, D, S, W$ | total number of CBs, dispatchable, solar and wind DGs, respectively |
| $CB_{(c)}^{(min)}, CB_{(c)}^{(max)}$ | minimum and maximum number of capacitors in a CB |
| $CB_{(c,t)}^{(ON)}$ | number of capacitors switched-on in a CB at time $t$ |
| $f$ | probability distribution functions |
| $f_1, f_2$ | objective functions to be minimised |
| $I_{(i,j)}$ | current flowing between buses $i$ and $j$ |
| $I_{maxp}$ | current at maximum power point |
| $I_{sc}$ | short circuit current |
| $K_i$ | temperature coefficient value for current |
| $K_v$ | temperature coefficient value for voltage |
| $N$ | total number of buses |
| $n_R, n_L$ | right and left data points, respectively |
| $N_{total}$ | total number of PV modules |
| $P_{(i,t)}, Q_{(i,t)}$ | active and reactive loads connected to the bus $i$ at time $t$ |
| $P_r$ | rated capacity of a Wind turbine |
| $P_s$ | power generated from a PV panel |
| $s_{ird}$ | solar irradiance |
| $s_w, s_{ci}, s_{co}, s_r$ | current wind speed, cut-in wind speed, cut-out wind speed and rated wind speed, respectively |
| $T_{amb}$ | ambient temperature |
| $T_{cell}$ | temperature of a cell |
| $T_{not}$ | nominal operating temperature of a solar cell |
| $TSCB$ | total number of switching operations of CBs |
| $TSO$ | total number of switching operations of an OLTC |
| $V_{(i,t)}$ | voltage of the $i$-th DG bus at time $t$ |
| $V_{maxp}$ | voltage at maximum power point |
| $V_{min}, V_{max}$ | minimum and maximum value of voltage |
| $V_{oc}$ | open circuit voltage |
| $V_{ref}$ | reference voltage for an OLTC |

uncertainties in the wind and solar power outputs. Therefore, it is essential to implement an optimal voltage regulation scheme which operates in real-time. The implementation of a voltage regulation scheme in real-time can eliminate scheduling errors. In addition, it is the intrinsic nature of several DGs to, at times, have low output power. For the accurate modelling of non-dispatchable DGs, the stochastic modelling of wind speed data and solar irradiance data should also be performed.

In this study, a rigorous real-time optimal SCADA-based two stage coordination algorithm for the voltage regulation of active distribution networks is proposed. This scheme sets out a new criterion for the selection of tap positions using the optimisation algorithm in real-time. The new tap position of an OLTC is found using the $\mu$-GA. Both DSPDGs and non-dispatchable DGs are taken into account. DGs are classified into two groups. Some DGs are not permitted to change their active powers, whereas some can also alter their active powers for the voltage regulation. In the first stage, an OLTC changes its tap position, whereas in the second stage, an RGA is applied to find the optimal power factors of DGs and the number of capacitors to be switched on/off. As the variations in wind speed and solar irradiance increase the complexity of voltage regulation process, the intermittent nature of the DGs is also taken into account for evaluating the performance of the proposed scheme, and the real world wind speed and solar irradiance data are modelled for the simulations.

The significant contributions made by this study can be summarised as follows:

(1) *Real-time optimal coordination scheme:* The study proposes a rigorous optimisation-based coordination scheme for an OLTC, DGs and capacitor banks, which operates in real time.
(2) *New tap position:* A new $\mu$-GA-based methodology for the selection of the OLTC-tap is presented. The methodology considers the voltage violations for all the buses simultaneously.
(3) *Dispatchable and non-dispatchable DGs:* The proposed scheme considers not only the DSPDGs, but also performs efficiently with the non-dispatchable DGs.
(4) *Optimal parameters:* An RGA is used for the calculation of optimal parameters such as power factors, active powers of DGs and the number of switched on/off capacitors. The use of the RGA reduces the execution time of the simulations.
(5) *Intermittent DG outputs:* The real world data of wind speed and solar irradiance are modelled for wind DGs and PV panels. Intermittent DG outputs do not affect the performance of the proposed real-time voltage control algorithm. The scheme can tolerate the worst cases of high peak hours and small DG output powers.

### 1.2. Related work

An extensive body of literature on the subject of voltage regulation of DG-integrated distribution networks already exists. In [8–10], optimisation based algorithms were used for calculating

the DG outputs. An OLTC and capacitors' day-ahead switching schedules were also calculated in [8,9]. A particle swarm optimisation based network partitioning technique for the voltage regulation of a distribution system including the wind, solar and biomass DGs was developed in [11]. In [12], an online coordination between an OLTC and DSPDGs was carried out, and the optimisation problem was solved using the gradient descent algorithm. New control lines were installed for mitigating the voltage rise issues caused by the DGs in [13]. A sensitivity analysis based coordination scheme for the voltage control of a power system with wind farms was proposed in [14]. In [15], two SCADA-based schemes were proposed. The first scheme employs a rule-based coordination scheme between the OLTC and DSPDGs, whereas the second scheme uses an optimisation algorithm to find the optimal parameters such as the tap settings of the OLTC and the DSPDG-output set points. In [16], the presented algorithm divides the distribution network into two regions: one region is assigned to the OLTC for voltage regulation, and the DSPDG regulates the voltage of the second region; the scheme operates in real-time. In [17], the effects of network reconfiguration on voltage control schemes have been considered. Various control zones for DSPDGs were established, and the scheme operated in real-time. In [18], voltage regulation of a solar power DG integrated with the power system was conducted based on the coordination of electric vehicles with an OLTC. In [19], a day-ahead scheduling was carried out for non-dispatchable DGs using a harmony search optimisation algorithm. An adaptive voltage control scheme for the voltage regulation of distribution networks was proposed in [20]. In [21,22], DSPDGs changed their outputs after measuring the local voltages of DG buses. A two-stage voltage regulation scheme was proposed in [23]. In the first stage, dispatch schedules of capacitors were found, whereas in the second stage, an OLTC was used to control the voltage in real-time. A GA was employed in the first stage, whereas in the second stage, an OLTC changes its tap position by measuring the change from the reference voltage. Dynamic programming was used in [24], and the optimal tap positions and capacitor schedules were found for the next day. Because of the above studies, we have attempted to address all the issues related to the voltage regulation of active distribution networks in our proposed scheme.

The paper is organised as follows: Section 2 explains the fundamental nature of the problem. Section 3 introduces the proposed scheme. Section 4 describes the modelling of DSPDGs, wind speed data, wind DGs, solar irradiance data, PV panels and capacitor banks. A Savitzky-Golay filter is also presented in Section 4. Section 5 describes the test system and the simulation cases. Section 6 presents the results and discussion. Finally, the paper is concluded in Section 7.

## 2. Problem description

Fig. 1 shows the model of an active distribution network with an OLTC, a CB and various types of DGs. In traditional methods for voltage regulation, the voltage regulation point for an OLTC is fixed. It is a common practise to find this point by running a load flow program connecting all of the loads and disconnecting all of the capacitors from the power system. The input voltage level is set at 126 V (120 V base). After the execution of the load flow program, the point at which the voltage drops to 120 V is then selected as a regulation point [25]. The compensation circuit instructs the OLTC to select new tap positions under different conditions.

When the DGs are integrated into the distribution networks, some of the load currents, which were previously supplied by the substation, are now provided by the DGs. Because the compensation circuit calculates voltage drops by measuring the local current of the line, this situation affects the operation of the OLTC and manipulates the setting of the compensation circuit. It is impossible for the compensation circuit to operate accurately under high DG penetrations [26]. The parallel operations of various power devices may increase the switching operations of an OLTC due to the absence of coordination between them.

In the next section, we present our proposed scheme, which attempts to address all of the aspects of voltage regulation of active distribution networks and also meet the criteria set by the IEEE standard.
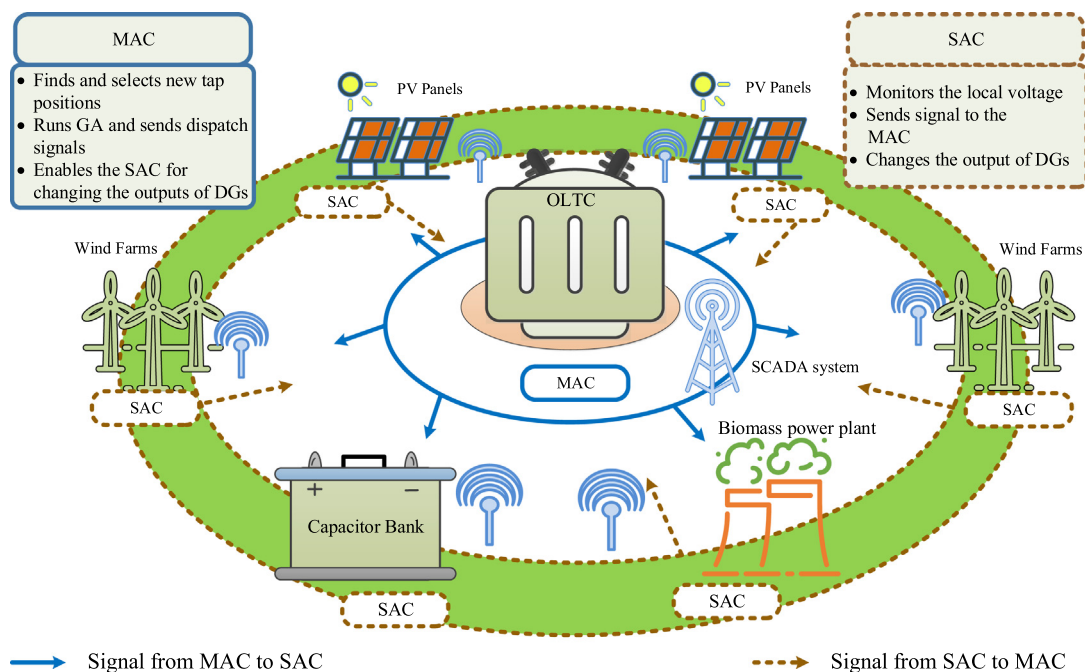


**Fig. 1.** Model of an active distribution network with an OLTC, DGs, a CB and an SCADA system.

## 3. Proposed voltage control algorithm

As explained in Section 1, the proposed voltage control algorithm is an SCADA-based algorithm, which is executed using the values obtained from the SCADA system. Voltages at the DG buses are locally monitored. The main algorithm is implemented with the assistance of controllers. Before explaining the necessary steps of the main algorithm, the basic operations of these controllers are presented as follows:

(1) The first type of controller, MAC, is installed near the relay of the OLTC. An MAC receives all of the voltage values of the DG buses sent by the SCADA system and determines the new tap position of the OLTC. If the output of the DG must be increased or decreased, the MAC establishes a connection with an SAC and sends the command to change the set point of the DG output. The MAC enables the SAC for a certain period of time, to alter the output of the DG. The SAC is not allowed to make the decision of changing the DG output by itself. Fig. 1 illustrates the communication between two controllers and presents their basic operations.

(2) The second type of controller, SAC, is installed at the DG buses. An SAC locally monitors the voltage of a DG bus. After receiving instructions from the MAC, it changes the output set points of a DG. Whenever the DG bus voltage crosses the feeder set limit, the SAC establishes a connection with the MAC and sends new voltage values for the DG bus to the MAC.

The different stages of the proposed algorithm are presented in the subsections below:

### 3.1. Stage-1: Tap settings of an OLTC

The problem of finding optimal operating conditions for an OLTC, CBs and DGs is a multi-variate optimisation problem. As the number of the DGs and capacitor banks in the distribution network increase, the variables in the optimisation problem also increase. For large power systems, it takes a significant amount of time to compute the optimal parameters due to the large number of decision variables, which makes it difficult to implement the optimisation algorithms in real-time. Usually, the delay time for an OLTC, before it operates, is 5 s. Owing to a large number of decision variables, the execution time for optimisation algorithms, to discover optimal parameters, becomes huge which makes the system unreliable because the OLTC must operate after 5 s. Instead of solving the problem as a whole block, if we split the problem into two, we can reduce the execution time of the algorithm to make the operation of the distribution system reliable. In Stage-1 of our proposed scheme, we only find the optimal tap positions, whereas in Stage-2, other parameters are found optimally by solving a large optimisation problem. The separation into two problems makes the tap calculation a univariate problem with a small search space, which eventually reduces the execution time of the optimisation algorithm.

Stage-1 is further divided into two sub-stages.

### 3.1.1. Classification

As explained above, whenever the voltage at the DG bus violates the defined set limits, an SAC notifies an MAC of the situation. After the MAC receives and records all of the voltages of the DG buses, the MAC categorises the DGs into two groups as shown in (1) and (2). The group $\Upsilon_1$ contains DGs that can only vary their power factors, whereas group $\Upsilon_2$ consists of DGs that can also alter their active power outputs. The conditions in (1) illustrate that we do not allow the optimisation algorithm to change the active powers of DGs. The DGs are identified by the identification constants $(\zeta_{(n)})$ assigned to them for preparing their groups. The identification constants $(\zeta_{(n)} = \Psi_1)$ are allocated to the variable power factor DGs, whereas the variable active power DGs are identified by the value $\zeta_{(n)} = \Psi_2$. It is important to mention that it is the choice of the DSO to decide DGs in groups $\Upsilon_1$ and $\Upsilon_2$.

$$\Upsilon_1(\zeta, PF, P) = DG_{(i)}^{(\zeta_{(i)})} \ \forall \ \zeta_{(i)} = \Psi_1, \Delta PF_{(i)} \neq 0, \Delta P_{(i)} = 0 \tag{1}$$

$$\Upsilon_2(\zeta, PF, P) = DG_{(i)}^{(\zeta_{(i)})} \ \forall \ \zeta_{(i)} = \Psi_2, \Delta PF_{(i)} \neq 0, \Delta P_{(i)} \neq 0 \tag{2}$$

The classification of DGs makes the proposed scheme universal in terms of dealing with all types of DGs. The costs of active powers provided by PV panels and wind power DGs are directly related to the customer benefits. The owners may not be willing to sacrifice their interests by curtailing active powers at the time of the voltage rise. Curtailing active powers reduces the amount of active power sold by the DG-owner, which results in a reduction of financial benefits for them. In that case, a DSO can categorise the DGs based on active power control capabilities of various DGs to maximise the benefits for DG-owners. Moreover, the cost of operation of some DGs such as the wind and solar DGs is small in comparison with other DGs such as biomass power plants and diesel generators. Therefore, the DSO can keep high-cost DSPDGs in group $\Upsilon_2$ to control their active powers for optimal operation of the distribution systems.

### 3.1.2. Optimisation for tap selection

Having classified the DGs, the MAC runs the optimisation algorithm, $\mu$-GA, to find the optimal tap position for an OLTC. A $\mu$-GA is an optimisation algorithm which has a small population size. In a GA, the optimisation procedure begins by randomly generating a population of solutions. Next, the fitness of each solution is evaluated, and the stopping conditions are verified. If the stopping conditions have not been satisfied yet, a GA performs its selection operation. In the selection process, solutions with the high fitness values are chosen to move to the next generation. Later, the crossover operation is performed on the newly selected solutions. In the crossover procedure, two parent solutions are selected at random from the population, and some of the portions of both solutions are mutually exchanged to create the offspring solutions. After this step, the mutation schemes are applied on the population. During the mutation, the solutions are perturbed to create new solutions. To avoid the high deterioration of the solutions, the probability of mutation is usually kept very small. During all these steps, best solutions, also known as elite solutions, are kept unchanged. Finally, the fitness of the new population is evaluated, and the same procedures continue until the stopping conditions are met [27]. In [28], it has been proved using Markov chain analysis that a GA with the elitism mechanism converges to the global optimum solution. Since the search space is small for tap position problem, we have employed the $\mu$-GA. The $\mu$-GA reduces the execution time of the algorithm and converges quickly to the global optimum solution.

The primary purpose of an OLTC in the conventional distribution network is to keep the voltage of the regulation point within safe operating limits. However, with the integration of numerous DGs with power systems, the selection of a new tap position based on a single regulation point is not beneficial because some DGs can experience a voltage rise, while some can experience a voltage drop. Therefore, to deal with both situations, we have formulated the problem of finding tap positions as the minimisation of mean squared error from the set point voltage in (3) for all the buses. The objective function, given in (3), is minimised to find the optimal tap position of an OLTC.

$$Min \ f_1(\lambda) = \frac{1}{N} \sum_{i=1}^{N} (V_{ref} - V_{(i,t)})^2 \qquad (3)$$

Changing the tap position considering the loss minimisation increases the voltage level of buses in the distribution networks, which results in a rise in the energy losses. However, the objective function found in (3) not only keeps the voltages of all the buses near the reference value of the voltage, but also reduces the energy losses of the system.

### 3.1.3. Constraints

Following constraints must also be satisfied by optimal solutions.

(a) *Voltage:* The *i*-th DG bus voltage should be within the minimum and maximum voltage limits.

$$V_{min} \leqslant V_{(i,t)} \leqslant V_{max} \qquad (4)$$

(b) *Tap Postion:* The generated tap position of an OLTC must lie within the maximum and minimum allowable range of the taps.

$$\lambda_{min} \leqslant \lambda_{(i,t)} \leqslant \lambda_{max} \qquad (5)$$

(c) *Power factor of DGs:* The power factors of the *i*-th PV panel, wind DG and DSPDG should not change from the previous time state value in Stage-1.
  (i) *PV Panels:*

$$\phi_s^{(t)} = \phi_s^{(t-1)} \ \forall \ s = 1,2\ldots S \qquad (6)$$

  (ii) *Wind Power DGs:*

$$\phi_w^{(t)} = \phi_w^{(t-1)} \ \forall \ w = 1,2\ldots W \qquad (7)$$

  (iii) *DSPDGs:*

$$\phi_d^{(t)} = \phi_d^{(t-1)} \ \forall \ d = 1,2\ldots D \qquad (8)$$

(d) *Active powers of DGs:* The change in active powers of PV panels, wind DGs and DSPDGs should be equal to zero in Stage-1.
  (i) *PV Panels:*

$$P_s^{(t)} - P_s^{(t-1)} = 0 \ \forall \ s = 1,2\ldots S \qquad (9)$$

  (ii) *Wind Power DGs:*

$$P_w^{(t)} - P_w^{(t-1)} = 0 \ \forall \ w = 1,2\ldots W \qquad (10)$$

  (iii) *DSPDGs:*

$$P_d^{(t)} - P_d^{(t-1)} = 0 \ \forall \ d = 1,2\ldots D \qquad (11)$$

(e) *Capacitor banks:* The state of *c*-th CB must remain similar to the previous time state value in Stage-1.

$$CB_{(c,t)}^{(ON)} = CB_{(c,t-1)}^{(ON)} \ \forall \ c = 1,2,\ldots,C \qquad (12)$$

Stage-1 presented above keeps the voltages of all the buses within recommended limits. Unlike conventional distribution networks, new tap positions are not found by measuring the voltages of one fixed regulation point: the voltage violations of all buses are taken into account for calculating the new tap position. Furthermore, solving the problem of tap selection as a single variable problem reduces the execution time of the optimisation algorithm, and the algorithm explained above operates in real-time for calculating the new tap position, which makes its implementation in real power systems uncomplicated and straightforward.

In the second stage, an MAC finds the optimal PFs and CB positions.

### 3.2. Stage-2: RGA and reactive power optimisation

Usually, it is assumed that the heuristic algorithms are slow, and they cannot be used in on-line control schemes. However, it is possible to enhance the on-line performance of a heuristic algorithm. In this study, we use a special heuristic algorithm, an RGA, which can be utilised in the on-line control schemes. In a conventional genetic algorithm, each time the algorithm is executed, new populations are generated. In contrast, an RGA does not create the whole new population every time. The last population, which was used for the calculation of an optimal solution, is stored in the memory. When the RGA is run again, instead of generating a new population, an RGA accesses the memory to acquire the stored population to run the RGA. Moreover, the performance of an RGA can be enhanced by setting and selecting different optimised parameters. The stopping criteria of an RGA can also be used to decrease the execution time of the algorithm.

In the first stage, the new tap position was selected. After instructing the relay of the OLTC to choose a new tap position, the MAC runs the RGA. In order to optimise the active and reactive powers of the distribution network, the RGA minimises the total power losses of the system. The objective function for Stage-2 is given in (13).

$$Min f_2(\mathbf{P}, \phi, \mathbf{CB}) = \frac{1}{2} \times \sum_{i=1}^{n} \sum_{j=1}^{n} G_{(ij)}$$
$$\times \left( (V_{(t,i)})^2 + (V_{(t,j)})^2 - 2 \times V_{(t,i)} \times V_{(t,j)} \times \cos(\delta_{(t,j)} - \delta_{(t,i)}) \right), \quad \forall t \qquad (13)$$

### 3.2.1. Constraints

Besides the conditions imposed in (1) and (2), optimal solutions provided by the RGA must also satisfy the following constraints imposed on the optimisation algorithm.

(a) *Voltage:* The voltage of the *i*-th DG bus should be within the minimum and maximum voltage limits.

$$V_{min} \leqslant V_{(i,t)} \leqslant V_{max} \qquad (14)$$

(b) *Current:* The magnitude of the current flowing in the line between buses *i* and *j* is calculated from (15). This current must be less than the maximum value of the allowable current in the power conductors.

$$I_{(ij)} = | Y_{ij} |$$
$$\times \left[ (V_i)^2 + (V_j)^2 - 2 \times V_i \times V_j \times \cos(\delta_j - \delta_i) \right]^{1/2} \qquad (15)$$

$$|I_{ij}| \leqslant I_{max} \qquad (16)$$

(c) *Power factor of DGs:* The power factors of the PV panels, wind DGs and DSPDGs should be within the minimum and maximum maintained limits of the PFs.
  (i) *PV Panels:*

$$\phi_s^{min} \leqslant \phi_s^{(i,t)} \leqslant \phi_s^{max} \forall s = 1,2\ldots S \qquad (17)$$

  (ii) *Wind Power DGs:*

$$\phi_w^{min} \leqslant \phi_w^{(i,t)} \leqslant \phi_w^{max} \ \forall \ w = 1,2\ldots W \qquad (18)$$

  (iii) *DSPDGs:*

$$\phi_d^{min} \leqslant \phi_d^{(i,t)} \leqslant \phi_d^{max} \ \forall \ d = 1,2\ldots D \qquad (19)$$

(d) *Active powers of DGs:* The active powers of the PV panels, wind DGs and DSPDGs categorised in different classes should obey various conditions given below based on their classes.

(i) *PV Panels:*

$$\Delta P_s^{(i,t)} = 0 \quad \forall \ \gamma_s^{(i)} \in \Upsilon_1 \tag{20}$$

$$P_s^{(min,i)} \leqslant P_s^{(i,t)} \leqslant P_s^{(max,i)} \quad \forall \ \gamma_s^{(i)} \in \Upsilon_2 \tag{21}$$

(ii) *Wind Power DGs:*

$$\Delta P_w^{(i,t)} = 0 \quad \forall \ \gamma_w^{(i)} \in \Upsilon_1 \tag{22}$$

$$P_w^{(min,i)} \leqslant P_w^{(i,t)} \leqslant P_w^{(max,i)} \quad \forall \ \gamma_w^{(i)} \in \Upsilon_2 \tag{23}$$

(iii) *DSPDGs:*

$$\Delta P_d^{(i,t)} = 0 \quad \forall \gamma_d^{(i)} \in \Upsilon_1 \tag{24}$$

$$P_d^{(min,i)} \leqslant P_d^{(i,t)} \leqslant P_d^{(max,i)} \quad \forall \gamma_d^{(i)} \in \Upsilon_2 \tag{25}$$

(e) *Capacitor banks:* The maximum number of switched on/off capacitors in a CB should be less than or equal to the total number of capacitors in a CB.

$$CB_{(c)}^{(min)} \leqslant CB_{(c,t)}^{(ON)} \leqslant CB_{(c)}^{(max)} \quad \forall \ c = 1, 2, \ldots, C \tag{26}$$

Having found the optimal solutions, the MAC sends signals to the SACs of the DGs and enables them for a certain period of time. The SAC selects the optimal solutions as the current set points of the DGs and CBs. After the allowed time has elapsed, the DG output variation terminal of the SAC is disabled again. Whenever the voltage of a DG bus violates the set limits, the SAC informs the MAC about the situation. All the actions are taken by the MAC to maintain the voltage of the system. Stage-2 of the proposed scheme is executed with the updated values of the variables, acquired from Stage-1. In this way, the conflict between two stages cannot take place.

Because the violations in the set limits of voltage initiate the steps performed in the proposed scheme, the execution of the scheme does not depend on the number of power devices in the system. If the scheme is implemented in a distribution network with only DGs or with only CBs, no changes will be required further in the main procedure. The optimisation algorithm in Stage-2 will find those solutions which minimise the objective function globally and meet the constraints at the same time.

Fig. 2 illustrates the steps performed in the proposed algorithm using a flowchart representation.
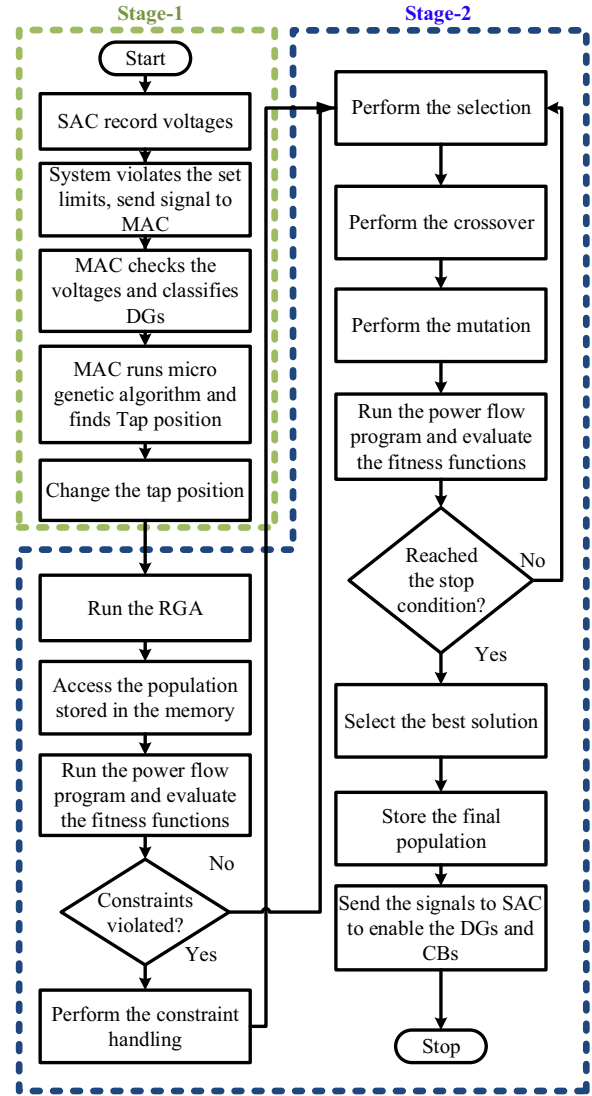
### 3.2.2. Switching operations

During the execution of simulations, the total number of switching operations of various devices are also calculated.

(i) *OLTC:* The total switching operations of an OLTC are found using (27).

$$TSO = \sum_{t=1}^{T} \left( \lambda_{(t-1)} \veebar \lambda_{(t)} \right) \tag{27}$$

(ii) *Capacitor banks:* The total switching operations of CBs are obtained using (28).

$$TSCB = \sum_{t=1}^{T} \left( CB_{(c,t-1)}^{(ON)} \veebar CB_{(c,t)}^{(ON)} \right) \tag{28}$$

### 3.2.3. Voltage quality

To evaluate the performance of the proposed scheme, percentage steady state voltage fluctuations (PSVFs) of the DG-buses are also found using (29) [24].

$$PSVF_{DGbus} = \frac{1}{T} \sum_{t=1}^{T} \left( |V_{(i,t-1)} - V_{(i,t)}| \right) \times 100\% \tag{29}$$



**Fig. 2.** Flowchart of the proposed algorithm.

## 4. Models of renewable energy resources

In this section, the modellings of the wind speed data, solar irradiance data, wind DGs, PV panels, DSPDGs and capacitor banks are presented, which are used in this study.

### 4.1. DSPDGs

The DSPDGs are considered as the source of firm power generation in this study. The net active power ($P_n^{(i)}$) at bus *i*, given in (30), is equal to the difference of active power load ($P_l^{(i)}$) and active power ($P_d^{(i)}$) provided by the DSPDG connected to the bus *i*. The net reactive power ($Q_n^{(i)}$) is also calculated similarly using (31). Owing to the facility of consuming and supplying reactive power, usually, synchronous generators based machines are used as the DSPDGs. Eq. (31) illustrates the reactive power control capabilities of the DSPDGs.

$$P_n^{(i)} = P_l^{(i)} - P_d^{(i)} \tag{30}$$

$$Q_n^{(i)} = Q_l^{(i)} \pm Q_d^{(i)} \tag{31}$$

### 4.2. Wind Power DGs

In literature, Weibull probability distribution is often used to model the variations in the wind speed [29]. The probability density function of the distribution above is given in (32).

$$f(s_w|a,b) = \begin{cases} \frac{b}{a^b} s_w^{b-1} e^{-(s_w/a)^b} & \text{for } x > 0 \\ 0 & \text{for } x \leqslant 0 \end{cases} \tag{32}$$

where $a$ and $b$ are the scale and shape parameters of the Weibull distribution, respectively. First, these parameters need to be estimated from the given wind speed data. We have used the MLE method for the estimation of parameters in this paper. Later, MCS are executed to generate the samples from the Weibull distribution. Finally, the wind DG-model given in (33) is used for obtaining electrical energy from the generated wind speed data [29].

$$P_w = \begin{cases} P_r \times \frac{s_w - s_{ci}}{s_r - s_{ci}} & \text{for } s_{ci} \leqslant s_w \leqslant s_{co} \\ P_r & \text{for } s_r \leqslant s_w \leqslant s_{co} \\ 0 & \text{otherwise} \end{cases} \tag{33}$$

### 4.3. PV panel modelling

For modelling the variations in the solar irradiance, the beta distribution is usually used [30]. For $\alpha, \beta > 0$, the pdf of Beta distribution is given as (34).

$$f(s_{ird}|\alpha,\beta) = \begin{cases} \frac{\Gamma(\alpha+\beta)}{\Gamma(\alpha)\Gamma(\beta)} \times s_{ird}^{(\alpha-1)} \\ \times (1 - s_{ird})^{(\beta-1)} & \text{for } 0 \leqslant s_{ird} \leqslant 1 \\ 0 & \text{for } s_{ird} < 0 \end{cases} \tag{34}$$

where $\Gamma$ is the gamma function; $\alpha$ and $\beta$ are known as the shape parameters of the beta distribution. For the parameters' estimation from the given solar irradiance data, we again use the MLE method. After that, MCS are employed for generating samples from the distribution. The model of a PV panel given in (35)–(39) provides electric power obtained from the generated solar irradiance samples [30].

$$T_{cell} = T_{amb} + \left( s_{ird} \times \frac{T_{not} - 20}{0.8} \right) \tag{35}$$

$$I = s_{ird} \times (I_{sc} + K_i \times (T_{cell} - 25)) \tag{36}$$

$$V = V_{oc} - K_v \times T_{cell} \tag{37}$$

$$\Lambda = \left( \frac{V_{maxp} \times I_{maxp}}{V_{oc} \times I_{sc}} \right) \tag{38}$$

$$P_s = N_{total} \times \Lambda \times V \times I \tag{39}$$

### 4.4. Savitzky-Golay filter

The real world data of wind speed and solar irradiance for a whole day have fewer variations in comparison with the data generated from MCS. For smoothing of the data generated from the MCS, a Savitzky-Golay (S-G) smoothing filter is used. In an S-G filter, smooth values ($y_s$) are obtained by fitting a polynomial shown in (40) through a fixed number of data points; a point, ($x_i$), is chosen, and the polynomial is fitted to the data points left and the right to the $x_i$ [31]. The polynomial is fitted by calculating constants ($b_k$) in the least squares sense by minimising (41).

$$P_i(x) = \sum_{k=0}^{M} b_k(x)^k \tag{40}$$

$$min\left( \sum_{j=i-n_L}^{i+n_R} (P_i(x_j) - y_j)^2 \right) \tag{41}$$

### 4.5. Capacitor banks

CBs are integrated with the distribution networks to provide the reactive power support for the voltage regulation. The net reactive power ($Q_n^{(i)}$) at bus $i$ after the placement of a CB is the difference of reactive load ($Q_l^{(i)}$) and the reactive power ($Q_c^{(i)}$) provided by the CB connected to the bus $i$ and is calculated using (42).

$$Q_n^{(i)} = Q_l^{(i)} - Q_c^{(i)} \tag{42}$$

In the next section, we present a test feeder and test cases considered for the simulations.

## 5. Test system and simulation cases

The proposed scheme has been tested on the IEEE 37-node test feeder shown in Fig. 3. Detailed specifications of the feeder can be found at [32]. We have made a few modifications in the original test feeder. In delta voltage regulators, changing one tap position affects two phases. For this reason, instead of using two open delta regulators, we replaced them with one three-phase close delta regulator for balanced voltage regulation. Also, two capacitor banks have been installed at Node-735 and Node-741, and three DGs with a single-phase power rating of 800 kW have been placed at three nodes, as shown in Fig. 3. The wind speed and solar irradiance summer data of six years (2007–2012) and seventeen years (1998–2014) have been taken for MCS [33,34]. Figs. 4a and b show the MCS generated data and S-G curves of the solar irradiance and wind speed data. A summer load curve of a distribution system in Seoul, Korea presented in Fig. 4c is used for the simulations. Moreover, the active powers of a PV panel and a wind DG are displayed in Fig. 4d., and the parameters of a PV panel and a wind turbine are given in Table 1. Only ±2 percent variation in the
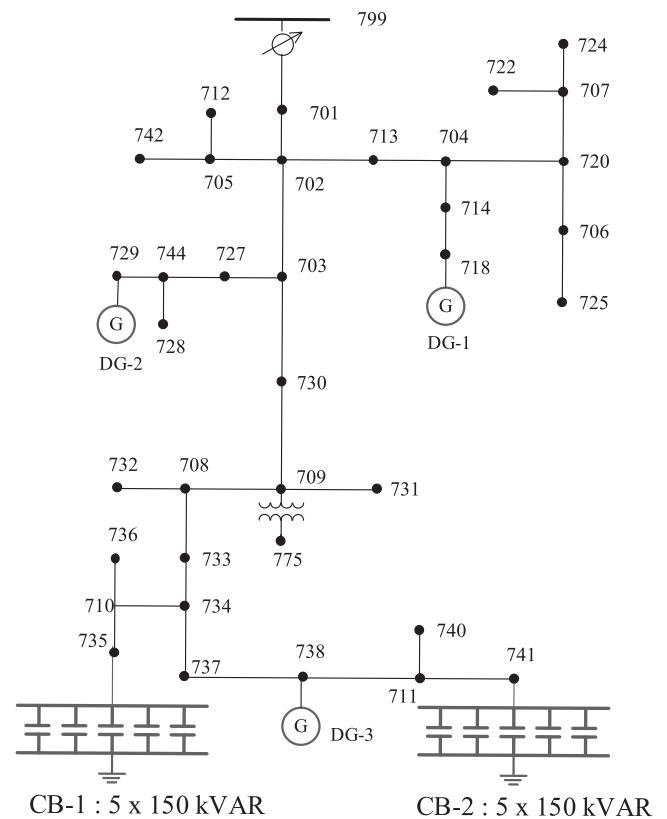


CB-1 : 5 x 150 kVAR　　　　CB-2 : 5 x 150 kVAR

**Fig. 3.** IEEE 37-node test feeder.

voltage is allowed in the simulation cases. However, for the large distribution networks with numerous DGs, the bandwidth of the operation may be widened to ±5 in accordance with [6]. The reference voltage set point for the OLTC has been kept at 1.0 p.u., and the DGs can change their power factors between 0.90 and 1 (both leading and lagging).

For the purpose of generality, node selections for DG placements are made by generating samples from the uniform probability distribution given in (43) using MCS with constraints (44)–(46) [35,36]. One hundred thousand samples were generated; the final set of outcomes has been selected for the DG placements. Nodes 718, 729, and 738 were selected for the DG installations.

$$f(\alpha) = \frac{1}{b-a} \quad \forall \quad \alpha \in [a,b] \tag{43}$$

$$\alpha_n + 5 < \alpha_{n+1} < \alpha_n - 5 \tag{44}$$

$$\alpha_n + 5 < \alpha_{n+2} < \alpha_n - 5 \tag{45}$$

$$\alpha_{n+1} + 5 < \alpha_{n+2} < \alpha_{n+1} - 5 \tag{46}$$

Four different test cases have been considered for the study. In the first test case, only PV panels of rating 800 kWs have been placed in the distribution network; the PV panels are permitted to change their PFs only with the CBs. In the second test case, doubly fed induction generators (DFIG)-based wind power DGs of rating 800 kWs have been installed in the test system; the wind power DGs are also allowed to change their PFs only along with the CBs. In the third test case, the performance of the proposed
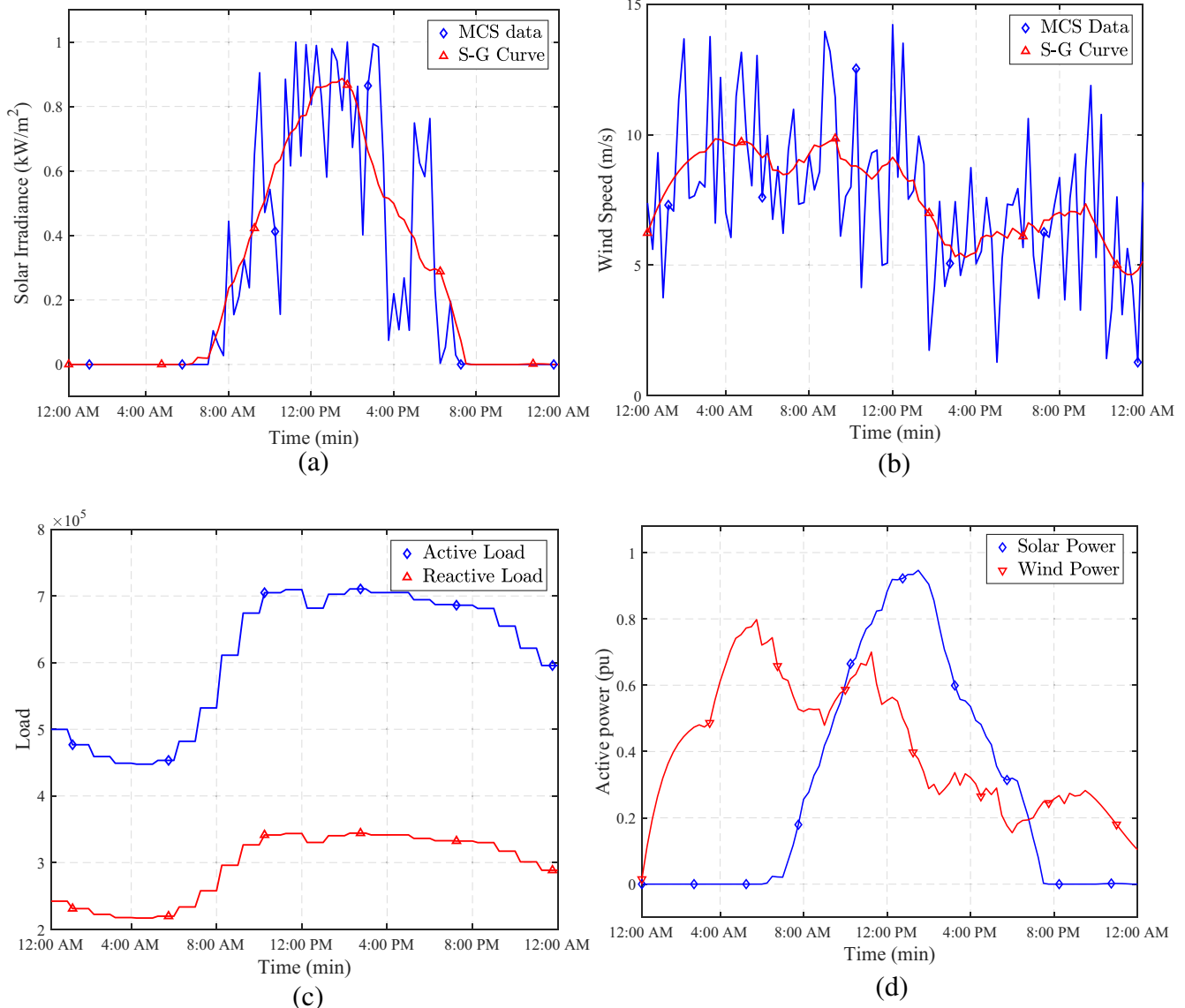
**Table 1**
Parameters of a PV module and a wind turbine.

| Characteristics | Units | Values |
|---|---|---|
| *PV panel* | | |
| Watt peak | W | 75.00 |
| Open circuit voltage | V | 21.98 |
| Short circuit current | A | 5.32 |
| Voltage at maximum power | V | 17.32 |
| Current at maximum power | A | 4.76 |
| Voltage temperature coefficient | mV/°C | 14.40 |
| Current temperature coefficient | mA/°C | 1.22 |
| Nominal cell operating temperature | °C | 43.00 |
| *Wind turbine* | | |
| Cut-in speed | m/s | 4.00 |
| Rated speed | m/s | 14.00 |
| Cut-out speed | m/s | 25.00 |



**Fig. 4.** (a) Solar irradiance curves, (b) wind speed curves, (c) load curves of a summer day, (d) active powers of solar and wind power DGs.

scheme has been evaluated with the DGs of different types and ratings. Two PV panels of power ratings 700 and 800 kWs and one wind DG of power rating 600 kW have been installed in the test system. Finally, in the fourth test case, the proposed algorithm has been tested by connecting two DSPDGs of power rating 350 kWs at buses 725 and 732 with the already installed PV panels of rating 800 kWs; in this test case, optimal active power curtailments in real-time have also been calculated. The simulations have been run for 24-h with the time interval of 15-min. It has been assumed that the OLTC operates after the delay of 5 s. The maximum number of generations, function tolerance between two consecutive generations and the number of stall generations have been used as the stopping criteria for the $\mu$-GA and RGA.

In the next section, the results for the test cases discussed in this section are presented.

## 6. Results and discussion

As explained in the preceding section, in Case-1, three PV panels were installed in the distribution network. Fig. 5 illustrates the results for this case. Fig. 5a shows that at the start of the

simulation, the voltage of the power system was below the set limit. The controllers (SACs) installed at the DG buses noted this decrease in the voltage and sent signals to the MAC. In Stage-1, after classifying the DGs into groups, the MAC executed the tap calculation algorithm and selected a new tap position using a $\mu$-GA. The DGs were not permitted to change their outputs. After the MAC changed the tap position of the OLTC, in Stage-2 of the proposed scheme, the MAC runs the RGA to find the optimal PFs. Having determined the optimal solutions, the MAC sent signals to the SACs. It can be noticed from Fig. 5d that the CBs were switched on. Near 12:00 PM, when the PV panels generated the maximum power, the voltage at the DG buses exceeded the upper limit. Again, the SACs sensed this increase in the voltage and sent the signals to the MAC. The MAC executed the both stages of the algorithm. First, the tap position was changed. Later, PFs of the PV panels shown in Fig. 5c were changed. Also, the switching happened in the CBs. During the night hours, the outputs of PV panels were again zero. However, it is clear from Fig. 5a that the proposed algorithm effectively kept the voltages of the DG buses within safe limits by changing the tap positions and dispatching the optimal schedule in real-time.
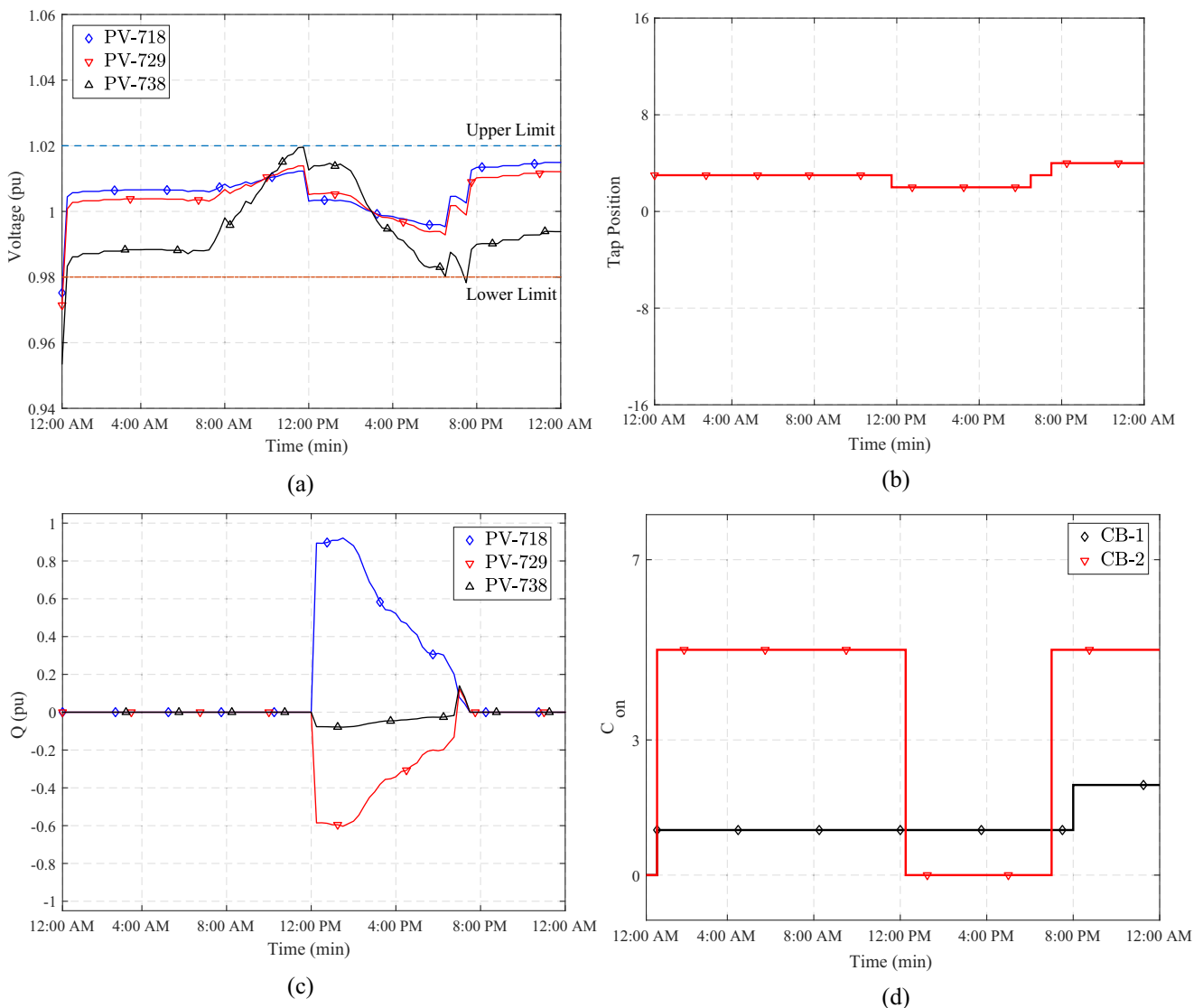


**Fig. 5.** (a) Voltage curves of the PVs, (b) tap position curve, (c) reactive powers of the PV panels, (d) switched on/off CBs.

In Case-2, three DFIG-based wind power DGs were placed in the test system. Fig. 6 shows the results obtained for this case. Fig. 6a indicates that at the start of the simulation, the voltage of the power system was below the set limit. The controllers (SACs) installed at the DG buses noted this decrease in the voltage and sent signals to the MAC. After making the groups, the MAC implemented the first stage of the proposed scheme. It can be seen from Fig. 6b that the OLTC changed its tap position. Having changed the tap position, in Stage-2 of the scheme, the MAC executed the RGA to find the optimal PFs and CBs positions. Fig. 6d illustrates that the CBs have changed their positions. After 4:00 AM, rise in the voltages of the DG-buses can be noticed due to the reduction in the load. The SAC again established the connection with the MAC and sent the current voltages of the buses. After receiving the voltages, the MAC performed the execution of the scheme. The improvement in the voltage profile can be seen in Fig. 6a. Despite the fluctuations in the wind speed and varying loads, results plotted in Fig. 6 show that the voltage profile of the system was within recommended limits.

In Case-3, the performance of the scheme was validated with different types and sizes of DGs. Two PV panels and a wind power

DG were placed in the test system. Fig. 7 shows the results obtained for this test case. It can be noticed from Fig. 7a that similar to other two cases, at the start of the simulation, the voltages were below the set limit. The SACs notified the MAC about the situation. Thereafter, in the first stage of the algorithm, the tap position of the OLTC was changed. After bringing the voltages into safe operating limits, in the second stage of the scheme, the MAC ran the RGA and changed the PFs of DGs and the position of CBs. The change in tap position, reactive powers and CBs can be observed in Fig. 7b, c, and d, respectively. Near 12:00 PM, the PV panels generated maximum output powers at their terminals, which resulted in an increase in the voltage of the system. It can be seen in Fig. 7 that again both stages of the proposed scheme were executed, and the voltages of the system were brought within safe operating limits.

In Case-4, the proposed algorithm was tested under the DG active power curtailment scenario; two DSPDGs were also placed in the test system. The active power set points of DSPDGs were calculated from the RGA. The results for this case are shown in Fig. 8. Similar to the other test cases, at the start of the simulations, the voltage of the system was below the set limits. After receiving the information from the SAC, the MAC implemented Stage-1 of
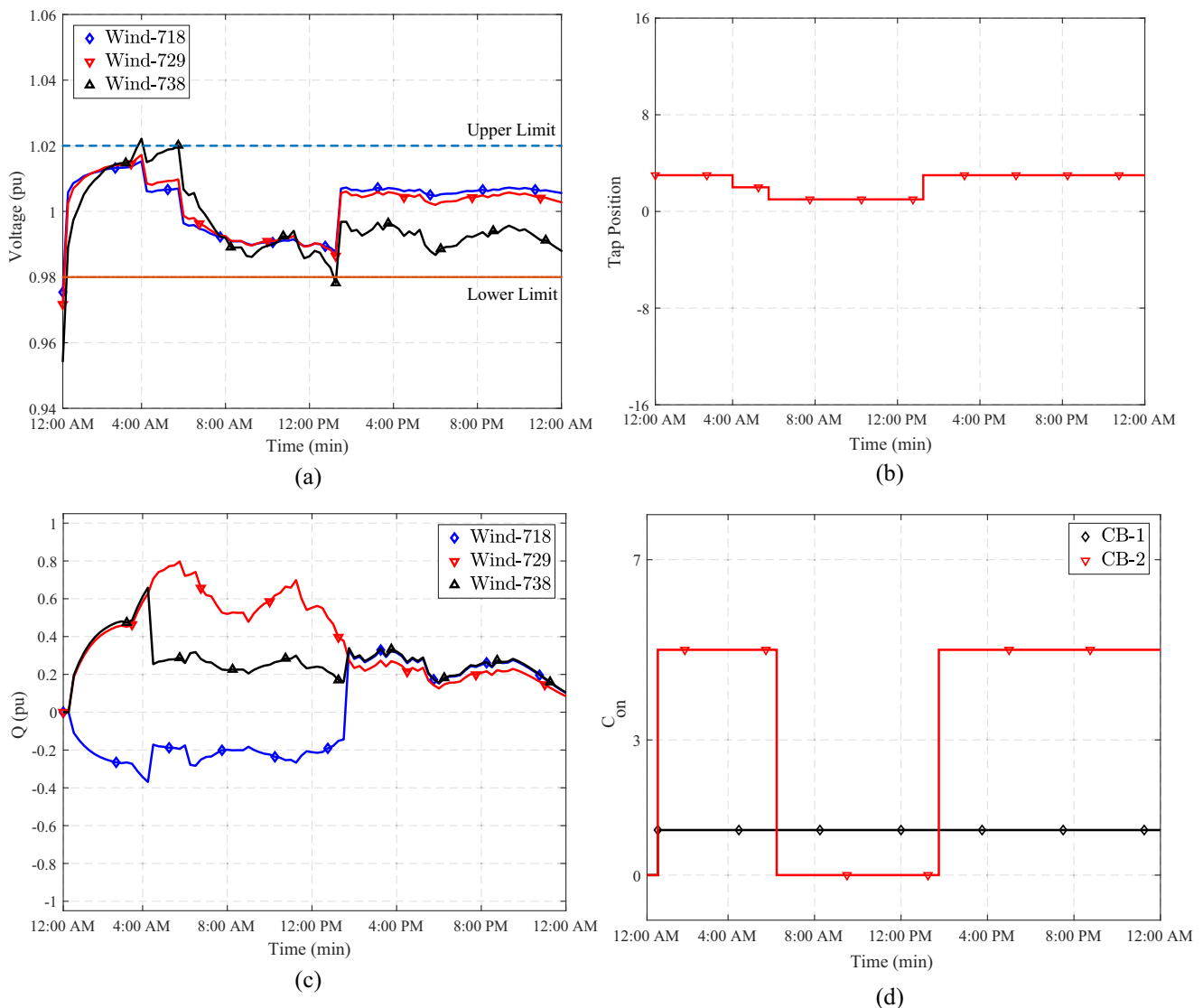


Fig. 6. (a) Voltage curves of the Wind DGs, (b) tap position curve, (c) reactive powers of the Wind DGs, (d) switched on/off CBs.
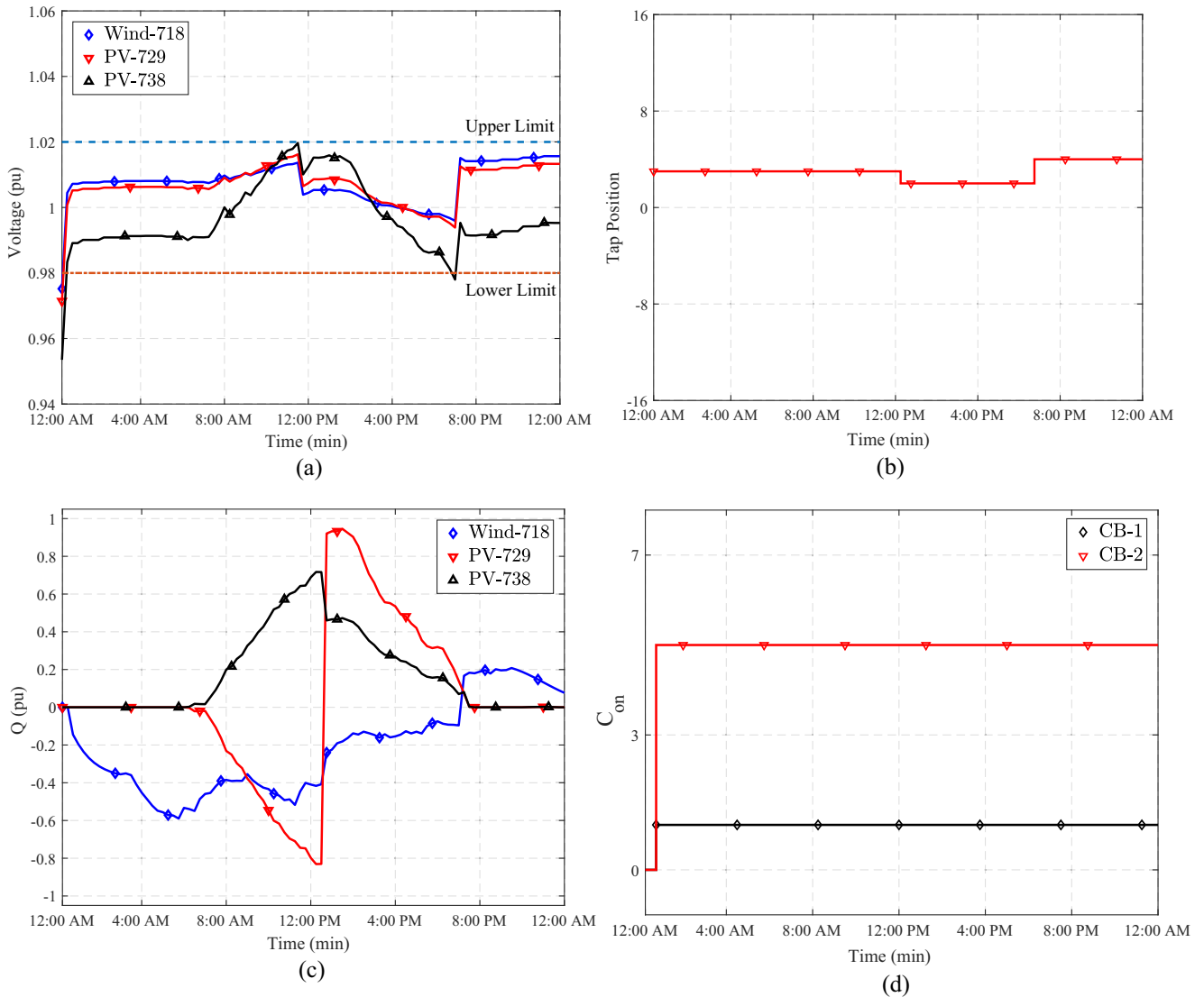
Fig. 7. (a) Voltage curves of the Wind DGs, (b) tap position curve, (c) reactive powers of the PV panels and wind DGs, (d) switched on/off CBs.

the scheme. It is interesting to note that unlike other test cases, in this case, both groups $\Upsilon_1$ and $\Upsilon_2$ contained DGs. The PV panels were kept in group $\Upsilon_1$, and the DSPDGs belonged to group $\Upsilon_2$. In the first stage, the MAC calculated and changed the tap position. In the second stage, after changing the tap position, when the MAC executed the RGA, the active power set points of the DSPDGs were also found. At the start of the simulation, the outputs of the DSPDGs were different, and the CBs were switched off. However, after changing the tap position, the MAC sent signals to DSPDGs to change their active powers, and the CBs were turned on at the same time. Fig. 8e shows the change in active and reactive powers of the DSPDGs. After 9:00 AM, due to increase in the output power of PV panels, the voltage of the system started rising. When the voltage exceeded the upper limit, due to the proposed scheme, the voltage of the system was brought to the set limit which is presented in Fig. 8a. It can be noticed that the tap position and PFs were changed. After 6:00 PM, the voltage again dropped because of the declined output of the PV panels. The new tap position and active power set points were calculated and changed again due to the violation of the voltage set limit. All the results presented in Fig. 8 explicitly show that the proposed scheme not

only optimises the reactive power of the distribution network, but also controls the active power of DGs. It can also be noticed from all the results that the conflict between the two stages of the proposed scheme did not take place. The scenario discussed in Case-4 can be used to reduce the operating cost of distribution networks. At this stage, it should be mentioned that the DGs were already present in the distribution system. The proposed methodology only found their optimal operating conditions by optimising the objective function. Moreover, in all the test cases, the power supplied by the grid can simply be computed by subtracting DGs power from the sum of loads and losses. The execution time of the optimisation algorithm in Stage-1 for all the test cases was between $2.3 \pm 0.2$ s.

Table 2 shows the energy losses of the test system and the number of switching operations of the OLTC and CBs for all the test cases. Because the PV panels do not provide powers at night, the losses are high in Case-1. Finally, the PSVF values are plotted in Fig. 9, and Table 3 provides the comparison between the PSVF-values obtained from the proposed scheme and the values obtained from two already published day-ahead scheduling schemes. It can be seen that all the values obtained from the pro-
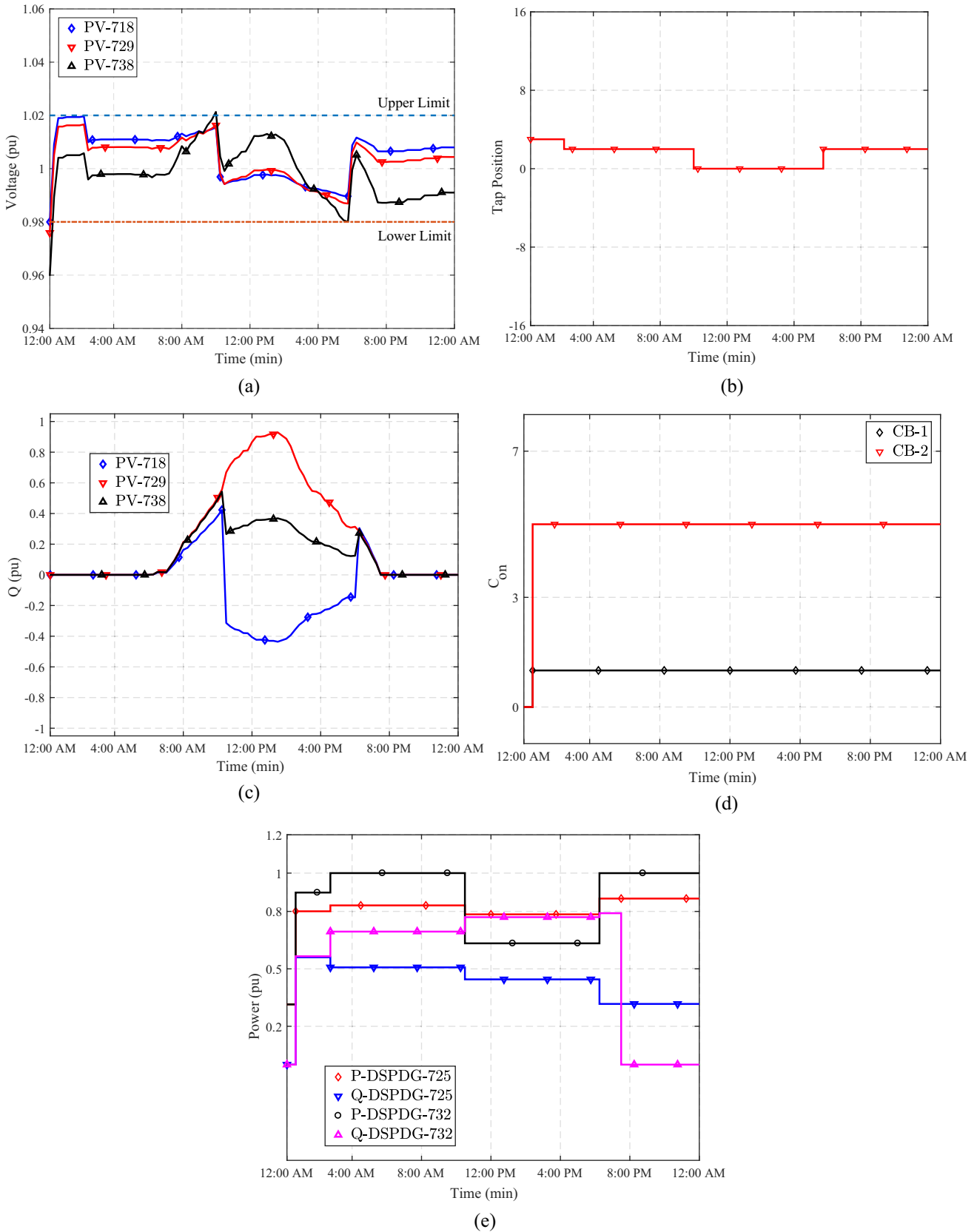
**Fig. 8.** (a) Voltage curves of PVs, (b) tap position curve, (c) reactive powers of the PV panels, (d) switched on/off CBs, (e) active and reactive powers of the DSPDGs.

posed real-time voltage regulation scheme are less than 0.2224 which proves that the performance of the proposed scheme regarding power quality is also considerable.

All the simulation cases and their results have confirmed that the proposed scheme operates correctly in various scenarios of real power systems.

**Table 2**
Results obtained for all the test cases.

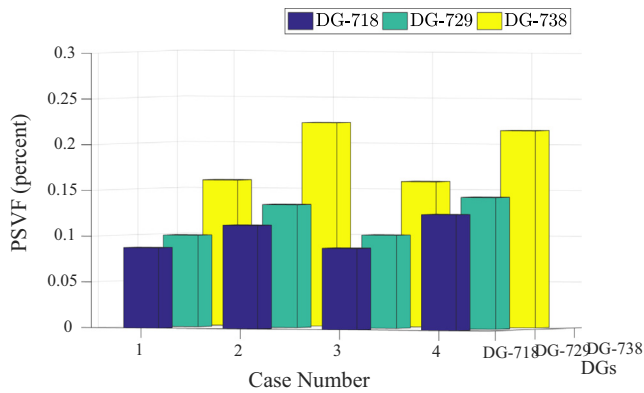| Parameter | Case 1 | Case 2 | Case 3 | Case 4 |
|---|---|---|---|---|
| Losses (MW h) | 8.8 | 6.4 | 8.6 | 3.5 |
| OLTC operations | 3 | 4 | 3 | 4 |
| CB1 operations | 2 | 1 | 1 | 1 |
| CB2 operations | 15 | 15 | 5 | 5 |
| Total operations | 20 | 20 | 9 | 10 |



**Fig. 9.** Percentage steady state voltage fluctuation values for DG-buses.

**Table 3**
Comparison of PSVF values obtained from different schemes.

| References | Stochastic modelling | Wind DGs | PV panels | PSVF values |
|---|---|---|---|---|
| [8] | Yes | Yes | No | 0.4900–1.030 |
| [24] | No | Yes | No | 0.4500–1.000 |
| Proposed scheme | Yes | Yes | Yes | 0.0878–0.2224 |

## 7. Conclusion

In this paper, a real-time optimal coordination scheme for voltage regulation of active distribution networks was presented. Major contributions of this research were as follows: a real-time optimal coordination scheme was proposed, a new method for the new tap selection was introduced, an on-line genetic algorithm was applied for the optimal parameter calculations, solutions for intermittent DG outputs were presented. The proposed scheme was tested and verified using its implementation on the IEEE 37-node feeder. Four test cases were considered. In Case-1, only PV panels and CBs were installed. In Case-2, wind power DGs and CBs were installed, and in Case-3, both PV panels and a wind DG were placed in the test system. Finally, in Case-4, DSPDGs were also placed with already installed PV panels and CBs. All the results plotted proved that the scheme operated efficiently, and the voltages of the buses were within safe operating limits. The PSVF-plot demonstrated that the voltage quality was enhanced, and the execution time of the optimisation algorithm was reduced. Irregularities in the availability of the DGs' outputs did not affect the performance of the proposed algorithm. In summary, the implementation of the proposed algorithm in real-world power systems can reduce the complexity of the voltage regulation process of power systems that include OLTCs, CBs and multiple DGs. Thus, the integration of DGs into a distribution network can be improved.

## Acknowledgement

## References

[1] Renewable electricity futures study volume 1: exploration of high-penetration renewable electricity futures. <http://www.nrel.gov/docs/fy12osti/52409-1.pdf>.
[2] Ma J, Wang X, Zhang Y, Yang Q, Phadke A. A novel adaptive current protection scheme for distribution systems with distributed generation. Int J Electr Power Energy Syst 2012;43(1):1460–6. http://dx.doi.org/10.1016/j.ijepes.2012.07.024.
[3] Zayandehroodi H, Mohamed A, Shareef H, Farhoodnea M. A novel neural network and backtracking based protection coordination scheme for distribution system with distributed generation. Int J Electr Power Energy Syst 2012;43(1):868–79. http://dx.doi.org/10.1016/j.ijepes.2012.06.061.
[4] Coster EJ, Myrzik JMA, Kruimer B, Kling WL. Integration issues of distributed generation in distribution grids. Proc IEEE 2011;99(1):28–39. http://dx.doi.org/10.1109/JPROC.2010.2052776.
[5] Tamp F, Ciufo P. A sensitivity analysis toolkit for the simplification of MV distribution network voltage management. IEEE Trans Smart Grid 2014;5(2):559–68. http://dx.doi.org/10.1109/TSG.2014.2300146.
[6] IEEE application guide for IEEE std 1547(tm). IEEE standard for interconnecting distributed resources with electric power systems. IEEE Std 1547.2-2008; 2009. p. 1–217. doi:http://dx.doi.org/10.1109/IEEESTD.2008.4816078.
[7] Bollen M, Hassan F. Integration of distributed generation in the power system. In: IEEE press series on power engineering. Hoboken (New Jersey): John Wiley & Sons, Inc.; 2011.
[8] Kim YJ, Ahn SJ, Hwang PI, Pyo GC, Moon SI. Coordinated control of a DG and voltage control devices using a dynamic programming algorithm. IEEE Trans Power Syst 2013;28(1):42–51. http://dx.doi.org/10.1109/TPWRS.2012.2188819.
[9] Kim YJ, Kirtley JL, Norford LK. Reactive power ancillary service of synchronous DGs in coordination with voltage control devices. IEEE Trans Smart Grid 2017;8(2):515–27. http://dx.doi.org/10.1109/TSG.2015.2472967.
[10] Yu L, Czarkowski D, de Leon F. Optimal distributed voltage regulation for secondary networks with DGs. IEEE Trans Smart Grid 2012;3(2):959–67. http://dx.doi.org/10.1109/TSG.2012.2190308.
[11] Nayeripour M, Fallahzadeh-Abarghouei H, Waffenschmidt E, Hasanvand S. Coordinated online voltage management of distributed generation using network partitioning. Electric Power Syst Res 2016;141:202–9. http://dx.doi.org/10.1016/j.epsr.2016.07.024.
[12] Fallahzadeh-Abarghouei H, Nayeripour M, Hasanvand S, Waffenschmidt E. Online hierarchical and distributed method for voltage control in distribution smart grids. IET Gener Transm Distrib 2017;11:1223–32. 9.
[13] Jeong BS, Chun YH. Feeder loop line control for the voltage stabilization of distribution network with distributed generators. J Electr Eng Technol 2014;9(1):1–5.
[14] Zhao H, Wu Q, Guo Q, Sun H, Huang S, Xue Y. Coordinated voltage control of a wind farm based on model predictive control. IEEE Trans Sust Energy 2016;7(4):1440–51. http://dx.doi.org/10.1109/TSTE.2016.2555398.
[15] Kulmala A, Repo S, Jarventausta P. Coordinated voltage control in distribution networks including several distributed energy resources. IEEE Trans Smart Grid 2014;5(4):2010–20. http://dx.doi.org/10.1109/TSG.2014.2297971.
[16] Muttaqi K, Le A, Negnevitsky M, Ledwich G. A coordinated voltage control approach for coordination of OLTC, voltage regulator, and DG to regulate voltage in a distribution feeder. IEEE Trans Ind Appl 2015;51(2):1239–48. http://dx.doi.org/10.1109/TIA.2014.2354738.
[17] Ranamuka D, Agalgaonkar AP, Muttaqi KM. Online coordinated voltage control in distribution systems subjected to structural changes and DG availability. IEEE Trans Smart Grid 2016;7(2):580–91. http://dx.doi.org/10.1109/TSG.2015.2497339.
[18] Cheng L, Chang Y, Huang R. Mitigating voltage problem in distribution system with distributed solar generation using electric vehicles. IEEE Trans Sust Energy 2015;6(4):1475–84. http://dx.doi.org/10.1109/TSTE.2015.2444390.
[19] Sheng W, Liu Ky, Liu Y, Ye X, He K. Reactive power coordinated optimisation method with renewable distributed generation based on improved harmony search. IET Gener Transm Distrib 2016;10(13):3152–62. http://dx.doi.org/10.1049/iet-gtd.2015.1051.
[20] Yalla MVVS, Jauch ET, Craig AP. Coordinated adaptive distribution Volt/VAR controls. Transmission and distribution conference, 1999, vol. 2. IEEE; 1999. p. 740–5. http://dx.doi.org/10.1109/TDC.1999.756142.
[21] Li H, Li F, Xu Y, Rizy DT, Adhikari S. Autonomous and adaptive voltage control using multiple distributed energy resources. IEEE Trans Power Syst 2013;28(2):718–30. http://dx.doi.org/10.1109/TPWRS.2012.2213276.
[22] Robbins BA, Hadjicostis CN, Garcia ADD. A two-stage distributed architecture for voltage control in power distribution systems. IEEE Trans Power Syst 2013;28(2):1470–82. http://dx.doi.org/10.1109/TPWRS.2012.2211385.
[23] Park JY, Nam SR, Park JK. Control of a ULTC considering the dispatch schedule of capacitors in a distribution system. IEEE Trans Power Syst 2007;22(2):755–61. http://dx.doi.org/10.1109/TPWRS.2007.895168.
[24] Viawan FA, Karlsson D. Combined local and remote voltage and reactive power control in the presence of induction machine distributed generation. IEEE Trans Power Syst 2007;22(4):2003–12. http://dx.doi.org/10.1109/TPWRS.2007.907362.
[25] Kersting W. The modeling and application of step voltage regulators. In: Power systems conference and exposition, 2009. PSCE '09. IEEE/PES; 2009. p. 1–8. doi:http://dx.doi.org/10.1109/PSCE.2009.4840004.

[26] Baran ME, Markabi IME. A multiagent-based dispatching scheme for distributed generators for voltage support on distribution feeders. IEEE Trans Power Syst 2007;22(1):52–9. http://dx.doi.org/10.1109/TPWRS.2006.889140.

[27] Goldberg DE. Genetic algorithms in search, optimization and machine learning. 1st ed. Boston (MA, USA): Addison-Wesley Longman Publishing Co., Inc.; 1989.

[28] Rudolph G. Convergence analysis of canonical genetic algorithms. IEEE Trans Neural Networks 1994;5(1):96–101. http://dx.doi.org/10.1109/72.265964.

[29] Hetzer J, Yu DC, Bhattarai K. An economic dispatch model incorporating wind power. IEEE Trans Energy Convers 2008;23(2):603–11. http://dx.doi.org/10.1109/TEC.2007.914171.

[30] Atwa YM, El-Saadany EF, Salama MMA, Seethapathy R. Optimal renewable resources mix for distribution system energy loss minimization. IEEE Trans Power Syst 2010;25(1):360–70. http://dx.doi.org/10.1109/TPWRS.2009.2030276.

[31] Savitzky A, Golay MJE. Smoothing and differentiation of data by simplified least squares procedures. Anal Chem 1964;36(8):1627–39. http://dx.doi.org/10.1021/ac60214a047.

[32] Distribution test feeders. <http://ewh.ieee.org/soc/pes/dsacom/testfeeders/index.html>.

[33] Draxl C, Clifton A, Hodge B-M, McCaa J. The wind integration national dataset (wind) toolkit. Appl Energy 2015;151:355–66. http://dx.doi.org/10.1016/j.apenergy.2015.03.121. http://www.sciencedirect.com/science/article/pii/S0306261915004237.

[34] National solar radiation data base. <http://rredc.nrel.gov/solar/olddata/nsrdb/>.

[35] DeGroot M, Schervish M. Probability and statistics. Addison-Wesley; 2012.

[36] Rubinstein R, Kroese D. Simulation and the Monte Carlo method. 2nd ed. Hoboken (New Jersey): John Wiley & Sons, Inc.; 2008.